

VISCOUS FLOW SIMULATIONS OF COAXIAL ROTORS

Nana Obayashi, Chong Zhou, Lakshmi Sankar and JVR Prasad

School of Aerospace Engineering, Georgia Institute of Technology, Atlanta, GA 30332, USA

Jeewoong Kim

Advanced Rotorcraft Technology, Inc. Sunnyvale, CA 94085, USA

Abstract

Numerical simulations have been conducted for a coaxial rotor tested by Harrington. A wake capturing approach using a commercial Navier-Stokes solver, and a hybrid Navier-Stokes-Free Wake analysis, have been employed. The rotor was trimmed so that the upper and lower rotor torques are equal, cancelling each other. Comparisons with test data and other published data are presented for hover performance over a range of thrust settings. The tip vortex trajectories have also been examined. The hybrid method was computationally efficient and gave acceptable results for hover performance over a range of thrust settings, indicating that this approach is suitable for analysis and preliminary design of rotors. At higher thrust settings, the more costly wake capturing methods were found to be more accurate.

1. INTRODUCTION

Over the past few years, there has been a growing interest in the use of coaxial rotors for helicopters, with a separate propulsor for propulsion. The use of a coaxial helicopter removes the need for the tail boom and tail rotor. This makes the vehicle compact for a given payload. Retreating blade stall may be eliminated with the use of the advancing blade concept (ABC). These benefits should, however, be weighed against the structural requirements for the blades, the complex pitch control system, and increased hub drag compared to a single rotor system. An excellent review of the coaxial rotor aerodynamics is presented in Ref. 1.

There is a need to understand and model the aerodynamic, aeroacoustic, and aeroelastic characteristics of these rotor systems. Conventional comprehensive analyses do a very good job of modeling the performance of the coaxial rotors^{2,3,4,5,6}, and the interaction of the upper and lower rotor is modeled in these analyses primarily through the trailing wake structures. Vorticity and vortex particle transport equation solvers coupled to a lifting line representation of the coaxial rotor blades have also been employed^{7,8,9}. Additional work has also been done using physics based models, particularly CFD methods, to better understand the complex physical interaction between the upper and lower rotor^{10,11,12,13,14}.

Barbely et al have presented a survey of recent studies related to coaxial rotor phenomena¹⁵.

The present researchers have developed a physics based, computationally efficient, hybrid Navier-Stokes/free wake tool called GT-Hybrid for analyzing conventional and coaxial rotors^{16,17,18}. This tool complements comprehensive analyses and wake capturing Navier-Stokes analyses developed at NASA, U.S. Army, and by commercial firms. Validation of these tools have been done against wind tunnel and test data for a variety of configurations. Aeroelastic effects of the blades on the hover, forward flight, and maneuvering single rotor configurations are accounted for, by a loose coupling between the present hybrid CFD tools and comprehensive analyses.

The present hybrid methodology is formulated so that single and multi-rotor configurations, including coaxial and tandem rotors, may be readily modeled. Preliminary results for a coaxial rotor in hover, using this methodology, was presented in Ref. 18. Coaxial rotors in forward flight were studied in Ref. 12. In the present study, additional applications of this hybrid approach to a coaxial rotor configuration in hover are presented.

2. COMPUTATIONAL METHODOLOGIES

In this section, the Georgia Tech Hybrid Navier-Stokes Methodology is briefly described. Comparisons with a commercial CFD tool

called Star-CCM+ has been done as part of this present work. For this reason, this commercial tool is also described.

GT-Hybrid^{16,17,18} is a finite volume based three-dimensional unsteady viscous compressible flow solver. The flow is modeled by first principles using the Navier-Stokes Methodology. The Navier-Stokes equations are solved in the transformed body-fitted coordinate system using a time-accurate, finite volume scheme. A third-order spatially accurate Roe scheme is used for computing the inviscid fluxes and second order central differencing scheme is used for viscous terms. The Navier-Stokes equations are integrated in time by means of an approximate LU-SGS implicit time marching scheme. The flow is assumed to be turbulent everywhere, and hence no transition model is currently used. The solver accepts a user defined table of blade geometric and elastic deformations and deforms the computational grid. The temporal change in computational cell volume is accounted for, by explicitly satisfying the Geometric Conservation Law (GCL). The near wake region is captured inherently in the Navier-Stokes analysis.

The influence of the other blades and of the trailing vorticity in the far field wake are accounted for, by modeling them as a collection of piece-wise linear bound and trailing vortex elements. The use of such a hybrid Navier-Stokes/vortex modeling method allows for an accurate and economical modeling of viscous features near the blades, and an accurate “non-diffusive” modeling of the trailing wake in the far field.

The vortex model is based on a Lagrangian wake approach where a collection of vortex elements are shed from the rotor blade trailing edge and are convected downstream. The strength of the vortex elements is based on the radial gradient of bound circulation and the number of wake trailers chosen by the user. In case of a single trailer coming off the blade tip, the vortex strength is assumed to be peak bound circulation at the instance the vortex segment is generated. In forward flight, shed wake filaments are also released downstream of the computational domain outflow boundary.

The trailing and shed vortex filaments are propagated in time at a local velocity,

calculated as the induced velocity due to all vortex filaments plus the free-stream velocity. The induced velocity due to the free wake structure are also calculated at the N-S computational domain outer surface and are applied as inflow boundary condition at the front, top, and bottom boundaries. This specification of planar velocity field at the inflow boundaries allows the vortices to reenter the computational domain.

Figure 1 shows a schematic view of the Hybrid method employed in GT-Hybrid, depicting the Navier-Stokes domain around the blade-region, the wake captured inside the near-blade Navier-Stokes domain and part of the wake which is modeled as a Lagrangian free wake.

GT-Hybrid currently has the capability to use advanced turbulence models such as SA-DES and KES to compute the eddy viscosity. Although various turbulence models are available in the GT-Hybrid solver, SA-DES model was used in this study for computational efficiency.

This analysis is optionally loosely coupled to complementary computational tools, and works seamlessly with aeroelastic, aeroacoustic, and ice modelling analyses.

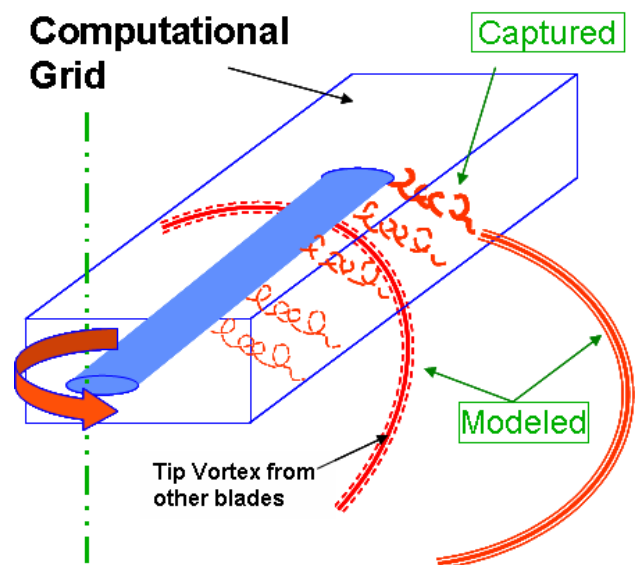


Figure 1. A Schematic View of the Hybrid Method

Because only the near field is computed using Navier-Stokes equations, the hybrid method is computationally very efficient. Typical CPU time for a given thrust setting varies between 4 and 6 hours for converged solutions

on a Linux cluster with 9 nodes (total of 72 cores), with message passing interface (MPI) calls used to exchange data between the individual nodes.

The wake-capturing simulations performed using STAR-CCM+ employ a density-based coupled flow solver that is based on the integral form of Navier-Stokes equations. In the present work, spatially second order central differences are used to estimate the inviscid fluxes. A second-order accurate time marching scheme, with dual-time sub-iterations, is employed. The solution was computed for 20 rotor revolutions to convect the starting vortex and initial transients that are an artifacts of starting the solution from quiescent flow, out of the flow domain. The air flow has been modeled as a compressible, ideal gas using the classical Reynolds-Averaged Navier-Stokes solver (RANS). The conservation equations for mass and momentum have been solved simultaneously with the coupled flow model, using implicit spatial integration in an unsteady analysis with a coupled algebraic multi-grid method. Menter's $k-\omega$ SST model has been used. Further details on the implementation are available in the documentation for STAR-CCM+. The physical time-step must be such that the Nyquist sampling criterion is satisfied, i.e., at least two time-steps per period must be sampled. A physical time step of 1-degree azimuth was used with 15 inner iterations which was found to be sufficient.

3. DESCRIPTION OF THE COAXIAL ROTOR CONFIGURATION

The Harrington coaxial rotors are modeled in present study¹⁹. Two-bladed, full-scale rotors inside a wind tunnel were tested at Langley full-scale tunnel in 1951. Table I below gives details of one of these configurations, commonly referred to as Rotor 2 configuration, modeled in this study.

In the experiments, the tests were carried out at two different tip speeds (327 feet/sec and 392 feet/sec). The present calculations were done only for the higher tip speed.

Table I. Harrington Rotor 2 Geometry

Parameter	Rotor 2
Number of Rotors	2
Number of Blades	2
Rotor Diameter, D	25 ft
Rotor Separation, h/D	2 ft (8% of D)
Root Cutout	20% R
Single Rotor Solidity, σ	0.076
Coaxial Rotor Solidity, σ	0.152
Airfoil	NACA four-digit symmetrical airfoil
Twist	untwisted

At the cutout (20%R), a NACA 0028 section was used. At the blade tip (100%), the blade section is NACA 0015. It was assumed that the thickness varies linearly between the cutout and the tip. An in-house grid generator was used to generate the body fitted grid for the near field surrounding the rotor blade, as shown in Figure 2.

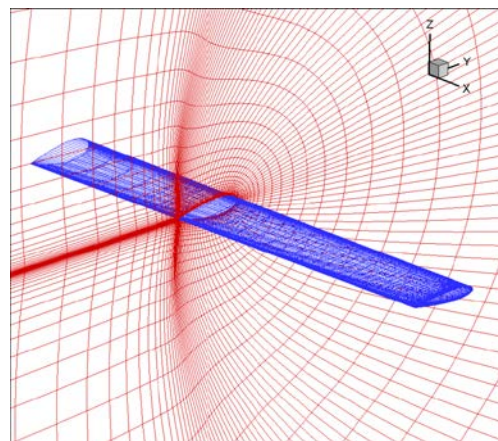


Figure 2. Body Fitted Grid for the Near Field

4. RESULTS AND DISCUSSIONS

In this section, selected results for Harrington Rotor 2 are presented. For each thrust setting, the rotor was trimmed within the GT-Hybrid analysis by adjusting the collective pitch of the upper and lower rotor so that the overall thrust coefficient was matched, and the net torque coefficient (sum of the torque on the upper and lower rotors) was zero. The wake capturing analysis (Star-CCM+) used the above trim settings based on the GT-Hybrid analysis.

Figure 3 show the computed and measured hover performance of the Harrington 2 rotor. Good agreement between the two analyses is found at low to moderate thrust settings. The GT-Hybrid solver slightly underestimated the figure of merit at lower thrust settings, and consistently overestimated the figure of merit at higher thrust settings. The wake capturing method performs significantly better at the higher thrust settings.

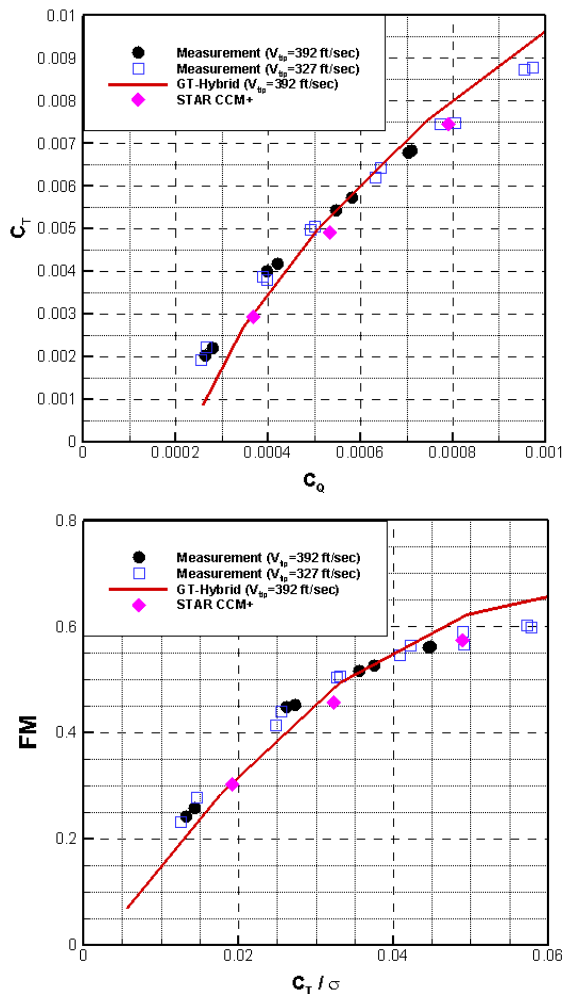


Figure 3. Hover Performance of the Harrington 2 Rotor

The contribution of thrust, and the corresponding power consumption, from the upper and lower rotors are also of interest. Because the rotor is trimmed for zero net torque, the upper and lower rotors consume equal amounts of power. Thus, the behavior of thrust was first examined. Because the test data only gives the overall rotor thrust, comparisons with test data are not feasible. However, comparisons with STAR-CCM+ could be made as shown in Figure 4. Very good agreement between the two sets of data is observed.

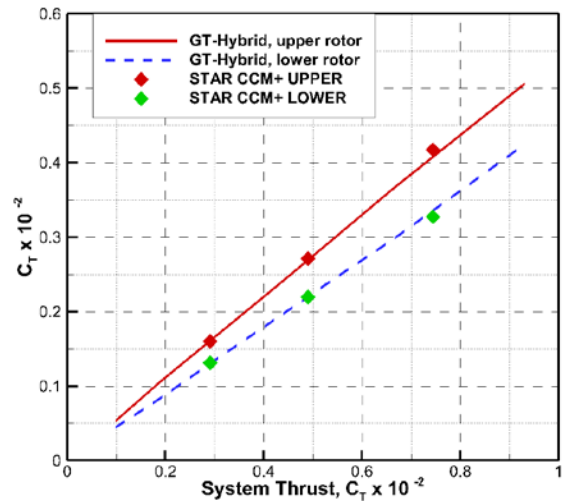


Figure 4. Contributions of the Upper and Lower Rotors to Overall Thrust

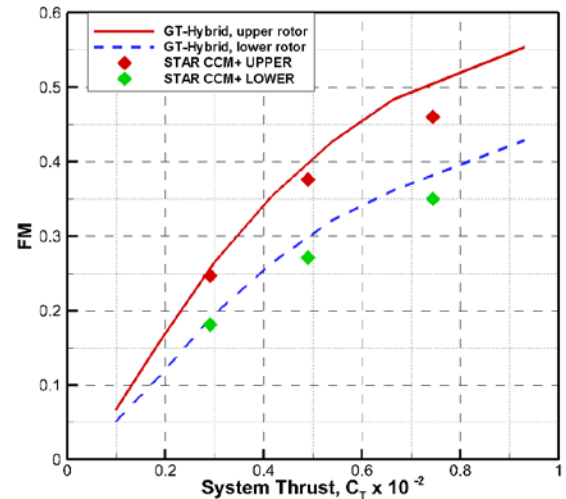


Figure 5. Figure of Merit for the Upper and Lower Rotors

It is seen that the upper rotor produces considerably more thrust compared to the lower rotor. The linear behavior of this curve suggests

that the division of labor between the upper and lower rotors is not affected by the thrust required, at least for the range of thrust settings considered. Since both rotors consume equal amounts of power, the figure of merit of the lower rotor would be expected to be lower than that of the upper rotor. This is indeed the case, as shown in Figure 5. CFD results from other researchers, e.g. Ref. 19, have also shown similar behavior.

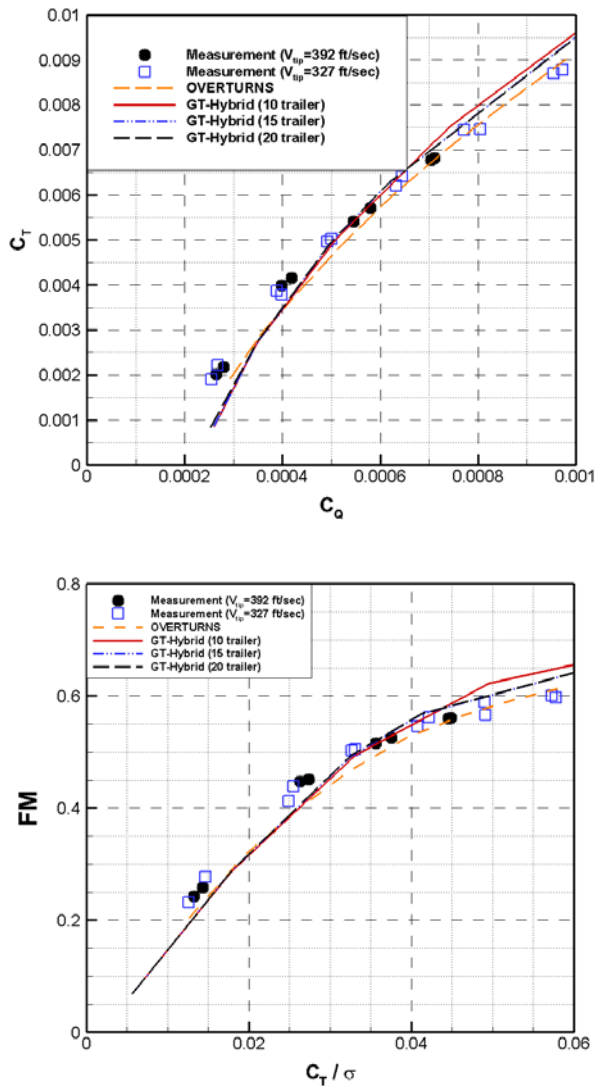


Figure 6. Effect of Number of Trailing Wake Filaments on Hover Performance

The inflow modeling may play a critical role in the prediction of power. The sensitivity of the GT-Hybrid predictions to free wake based inflow modeling was examined. The number of trailer elements was parametrically varied, and the number of times that the wake is updated per revolution of the rotor was also examined.

Figure 6 and Figure 7 show the predicted results. Comparisons with other published data²⁰ are also shown. Very small variations in the computed power and figure of merit are seen as these parameters are varied indicating that 10 trailers should be sufficient, with the wake filaments updated every 5 degrees of blade rotation.

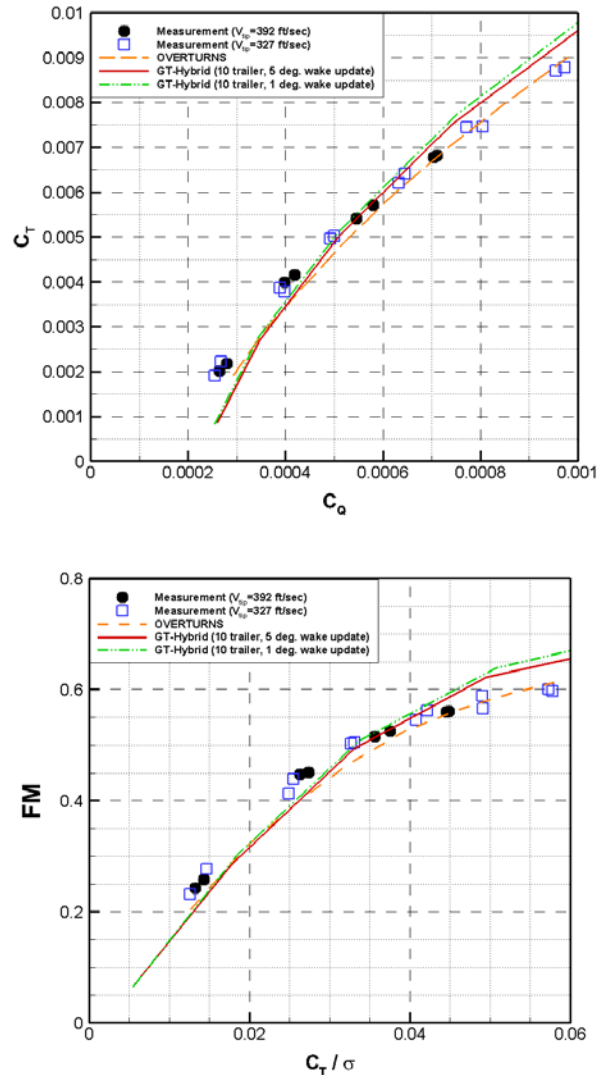


Figure 7. Effect of Wake Update on the Prediction of Hover Performance

Finally, the wake trajectories for the upper and lower rotor, as predicted by Gt-Hybrid and Star-CCM+ were examined. Figure 8 shows the vorticity contours from the wake capturing method at a thrust setting of 0.007. The locations of the peak local vorticity were identified and associated with tip vortex structures. As mentioned earlier, GT-Hybrid uses a free vortex method in the near field with

a prescribed far field trajectory model. Star-CCM+ uses a vortex capturing (Eulerian) method. As a result, correlation between the present method and others could only be achieved for the first 200 degrees of vortex age, when the vortex is coherent with a very small vortex core radius. At higher vortex ages, factors such as numerical diffusion and grid density begin to cause deviations.

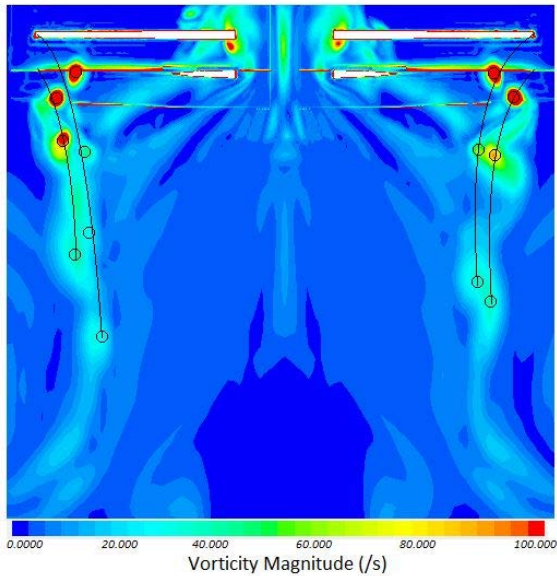


Figure 8. Tip Vortex Structures extracted from Star-CCM+ ($C_T=0.007$)

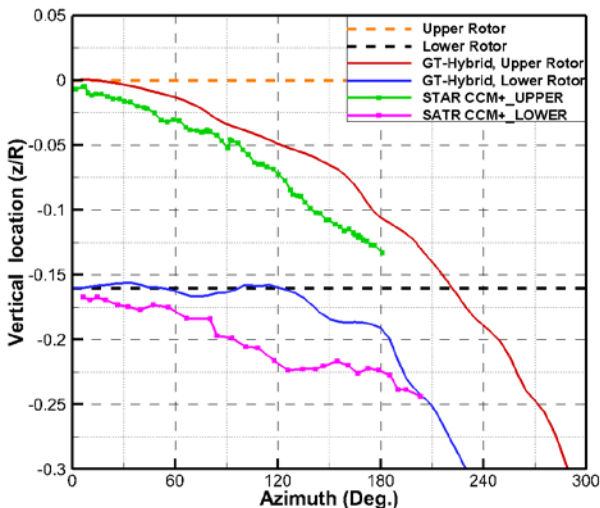


Figure 9. Tip Vortex Descent Rate as a Function of Wake Age ($C_T=0.007$)

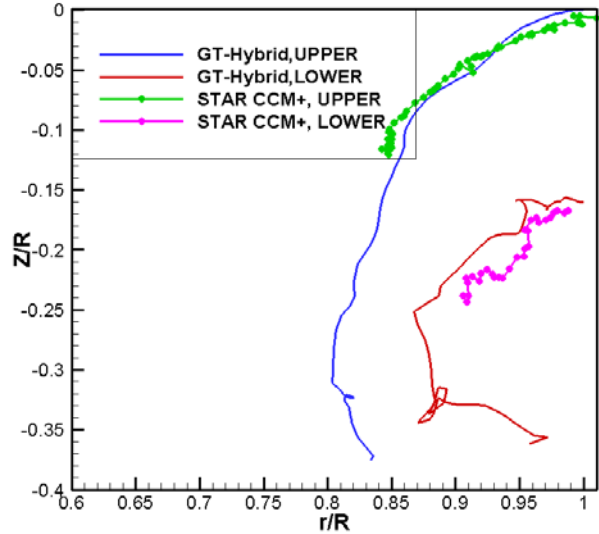


Figure 10. Tip Vortex Contraction Rate as a Function of Wake Age ($C_T=0.007$)

The hybrid method predicted a somewhat lower descent rate than the vortex capturing method at this thrust setting as seen in Figure 9. This indicates that the GT-Hybrid inflow velocity is lower than that for the wake capturing scheme at this thrust setting ($C_T=0.007$). As expected, the descent rate increases after the first blade passage of 180 degrees, for the upper and lower rotors, both.

Figure 10 shows the radial contraction of the tip vortices from the upper and lower rotors at the same thrust setting. Reasonable agreement between the hybrid method and the wake capturing methodology is observed. As expected, the higher thrust generated by the upper rotor leads to a greater contraction rate relative to the lower rotor. The tip vortex from the upper rotor interacts with the lower rotor at the radial position of approximately 85%R at this thrust setting.

5. CONCLUDING REMARKS

The aerodynamic behavior of a coaxial rotor system has been studied using two approaches – a hybrid Navier-Stokes-free wake solver, and a full wake-capturing approach. Comparisons with test data have been done. The performance of upper and lower rotors, for equal and opposite torque, was examined. Comparisons of the predicted vortex descent rate and radial contraction rate were also examined.

At lower thrust settings, both methods give good agreement with test data. As the thrust level increases, the hybrid method tends to underestimate the power required, and overestimate the figure of merit.

In terms of computational time, the hybrid method is very efficient, requiring 4 to 6 hours of CPU time on a Linux cluster with 72 cores of CPU. The wake capturing method is

considerably more expensive. For this reason, the hybrid method is well suited for initial design studies where the rotor geometry is parametrically varied, and quick reasonably accurate solutions are essential. Once a few promising configurations have been identified, more accurate (but computationally expensive) wake capturing simulations may be done to refine the design.

REFERENCES

- [1] Coleman, C. P., "A Survey of Theoretical and Experimental Coaxial Rotor Aerodynamic Research," NASA TP- 3675, March 1997.
- [2] Wachspress, D. A. and Quackenbush, T. R., "Impact of Rotor Design on Coaxial Rotor Performance, Wake Geometry and Noise," American Helicopter Society 62nd Annual Forum, Phoenix, AZ, May 9-11, 2006.
- [3] Lim, J. W., McAlister, K. W., and Johnson, W., "Hover Performance Correlation for Full-Scale and Model-Scale Coaxial Rotors," Journal of the American Helicopter Society, Volume 54, 2009.
- [4] Ho, J. C., Yeo, H., and Bhagwat, M., "Validation of Rotorcraft Comprehensive Analysis Performance Predictions for Coaxial Rotors in Hover," American Helicopter Society 71st Annual Forum, Virginia Beach, VA, May 5-7, 2015.
- [5] Schmaus, J. and Chopra, I. "Aeromechanics for a High Advance Ratio Coaxial Helicopter," American Helicopter Society 71st Annual Forum, Virginia Beach, VA, May 5-7, 2015.
- [6] Schmaus, J. and Chopra, I., "Performance and Loads Prediction for High Advance Ration Coaxial Rotor," AIAA SciTech Conference, Kissimmee, FL, January 2015, Paper AIAA-2015-1413.
- [7] Kim, Hyo Won and Brown, R. E., "A comparison of coaxial and conventional rotor performance". Journal of the American Helicopter Society, 2009.
- [8] Kim, H. W., Duraisamy, K., and Brown, R. E., "Effect of Rotor Stiffness and Lift Offset on the Aeroacoustics of a Coaxial Rotor in Level Flight," American Helicopter Society 65th Annual Forum, Grapevine, TX, May 27-29, 2009.
- [9] Zhao, J., and He, C., "Real-Time Simulation of Coaxial Rotor Configurations with Combined Finite State Dynamic Wake and VPM," American Helicopter Society 70th Annual Forum, Montreal, Canada, May 2014.
- [10] Lakshminarayanan, V., and Baeder, J., "High Resolution Computational Investigation of Trimmed Coaxial Rotor Aerodynamics in Hover", AHS International Specialists' Conference on Aeromechanics, San Francisco, CA, January 23–25, 2008.
- [11] Lakshminarayanan, V., "Computational Investigation of Micro-Scale Coaxial Rotor Aerodynamics in Hover," Ph. D Dissertation, University of Maryland, 2009.
- [12] Egolf, T. A., Rajmohan, N., Reed, E., and Sankar, L. N., "Hybrid CFD Method for Coaxial rotor Performance in Forward Flight," Proceedings of the 2010 AHS Aeromechanics Specialists Conference, San Francisco, CA, January 2010.
- [13] Juhasz, O., Sya, M., I Roberto Celi, Khromov, V., Rand, O., Ruzicka, G. C., and Strawn, R. C., "Comparison of Three Coaxial Aerodynamic Prediction Methods Including Validation with Model Test Data," Journal of the American Helicopter Society, Vol. 59, (4), 2010, pp. 366–381.
- [14] Singh, R. and Kang, H., "Computational Investigations of Transient Loads and Blade Deformations on Coaxial Rotor

Systems,” Paper AIAA 2015-2884, 33rd American Institute of Aeronautics and Astronautics Applied Aerodynamics Conference, Dallas, TX, June 22-26, 2015.

- [15] Barbely, N. L., Komerath, N. M., and Novak, L. A., “A Study of Coaxial Rotor Performance and Flow Field Characteristics,” AHS Technical Meeting on Aeromechanics Design for Vertical Lift, Fisherman’s Wharf, San Francisco, CA January 20–22, 2016.
- [16] Rajmohan, N., “Application of Hybrid Methodology to Rotors in Steady and Maneuvering Flight”, Ph.D. Dissertation, Georgia Institute of Technology, 2010.
- [17] Marpu R. P., Sankar L.N., Makinen S., Egolf T.A., Baeder J.D. and Wasikowski, M., “Physics Based Modeling of Maneuver Loads for Rotor and Hub Design,” Journal of Aircraft, 2014.
- [18] Kim, J., Sankar, L. N., and Prasad, JVR, “Application of a Navier-Stokes Free Wake Hybrid Methodology to the Harrington Coaxial Rotor,” AHS Technical Meeting on Aeromechanics Design for Vertical Lift, San Francisco, California, January 20–22, 2016.
- [19] Harrington, R. D., “Full-Scale-Tunnel Investigation of the Static-Thrust Performance of a Coaxial Helicopter Rotor,” NACA TN-2318, March 1951.
- [20] Lakshminarayan, V. K., and Baeder, J. D., “High Resolution Computational Investigation of Trimmed Coaxial Rotor Aerodynamics in Hover,” Journal of the American Helicopter Society, Vol. 54, (4), Oct. 2009.

holder of this paper, for the publication and distribution of this paper as part of the ERF proceedings or as individual offprints from the proceedings and for inclusion in a freely accessible web-based repository.

Copyright Statement

The author(s) confirm that they, and/or their company or organization, hold copyright on all of the original material included in this paper. The authors also confirm that they have obtained permission, from the copyright holder of any third party material included in this paper, to publish it as part of their paper. The author(s) confirm that they give permission, or have obtained permission from the copyright